

N_{γ} -Aryl glutamine analogues as probes of the ASCT2 neutral amino acid transporter binding site

C. Sean Esslinger,* Kimberly A. Cybulski and Joseph F. Rhoderick

NIH COBRE Center for Structural and Functional Neuroscience, Department of Biomedical and Pharmaceutical Sciences,
The University of Montana, Missoula, MT 59812, USA

Received 29 May 2004; revised 15 November 2004; accepted 15 November 2004
Available online 8 December 2004

Abstract—Analogues of L-glutamine were designed and synthesized to test a hydrogen-bond hypothesis between ligand and neutral amino acid transporter ASCT2. The key design feature contains a substituted phenyl ring on the amide nitrogen that contains electron withdrawing and electron donating groups that alter the pK_a of the amide NH. Through this study a preliminary binding site map has been developed, and a potent commercially available competitive inhibitor of the ASCT2 transporter has been identified. © 2004 Elsevier Ltd. All rights reserved.

1. Introduction

L-Glutamine is the most abundant free amino acid in mammalian blood plasma and cerebral spinal fluid.¹ As such an abundant bio-molecule, L-glutamine is involved in a variety of metabolic processes.² L-Glutamine is a major component of muscle,^{3,4} and in times of surgical illness has been classified as a ‘conditionally essential’ amino acid because of the increased metabolic requirements.⁵ As a precursor to TCA cycle intermediates, glutamine is an important source of energy.^{6,7} Glutamine acts as a vehicle for both carbon and nitrogen shuttling⁸ and serves as an excretion route for toxic ammonia.⁹ This systemic glutamine shuttling has been referred to as the glutamine cycle,³ and is also partly responsible for the pH buffering of the blood.¹⁰ Glutamine is also accepted as being a major metabolic precursor for the excitatory neurotransmitter L-glutamate¹¹ and the inhibitory neurotransmitter GABA.¹² In order for glutamine to participate in all of these roles, this small polar molecule must move throughout the body. It is this glutamine movement in which we are interested, and particularly transporter protein facilitated movement.

Neutral amino acid transporter proteins are responsible for facilitating movement of these highly polar solutes

across the lipophilic cellular membrane. A number of neutral amino acid transport systems have been identified, the main transport systems being the sodium dependent systems A, ASC, N, and the sodium-independent system L.^{13–15} As these transport systems are responsible for the translocation of the neutral amino acids (16 of the 20 common mammalian amino acids), one may suspect there is considerable overlap of substrate specificity. One common thread of these transport systems is that they all transport L-glutamine.

Our interest focused on system ASC glutamine transport (ASC for alanine, serine, cysteine). System ASC transport has been identified as an electroneutral obligate exchanger,¹³ and depending on transmembrane substrate ratios, it has the ability to operate in both influx and efflux directions.¹⁶ This transporter functions through a heteroexchange process, with glutamine efflux likely coupled to the influx of the system ASC substrates alanine, serine or cysteine.^{11,17} It has been proposed that the transporter ASCT2 (system ASC isoform 2) is responsible for part of the glutamine efflux from the astrocytes involved in the glutamine/glutamate cycling of glutamate neurotransmitter.^{11,15,17} The K_m reported for this transport process is in the range of 24–300 μ M for glutamine,^{18,19} has a lower throughput ($V_{max} \sim 8$ –15 nmol/min/mg)^{18,19} than system A or N activity, and has been proposed to contribute less of the overall glutamine glial efflux than system N.⁷ However, it was recently reported that a neuroblastoma cell line exhibits glutamine transport primarily due to system ASC.²⁰

Keywords: Pharmacophore; Modeling; Inhibition; H-Bonding.

* Corresponding author. Tel.: +1 406 243 5228; fax: +1 406 243 4713; e-mail: christopher.esslinger@umontana.edu

Similar glutamine transport activity reported in the literature occurs in the C6 rat glioma cell line and was further characterized as activity due to ASCT2.^{21,22} These observations could be the result of a general phenomenon of cancerous cells up-regulating ASCT2 mediated glutamine transport,²³ and exploitation of this phenomenon poses an attractive target for cancer research.^{24,25} Despite the increased interest in the ASCT2 transporter, little is known about the protein binding site and transport requirements other than the endogenous L-amino acid substrate profile (system ASC has a wide range of substrate neutral amino acids, from small to medium side chains). The goal of this study is to obtain information about the ligand-protein binding interactions and gain insight into the transport mechanism of the ASCT2 transporter.

Our study of the neutral amino acid transporter ASCT2 used the C6 rat glioma cell line as the model system. Our pharmacological analysis found the C6 cell line functionally exhibits glutamine uptake primarily by ASCT2 mediated transport (approximately 75% of total glutamine uptake, results not shown). The remaining 25% of glutamine uptake activity was consistent with system N and to a minor extent system L (these results were in the range of those reported independently).²¹ Uptake experiments were therefore performed in the presence of BCH (2-aminobicyclo-(2,2,1)heptane-2-carboxylic acid, a system L selective inhibitor) and at pH 6.0 (to eliminate the activity of system N) therefore isolating ASCT2 glutamine transport activity.

In agreement with reported results,²² we observed that glutamate was relatively inactive at inhibiting the uptake of radiolabeled L-glutamine at pH 7.4, but was a potent inhibitor at pH 6.0. This activity is hypothesized to come from the protonation of glutamate rather than from protonation of the protein, since the activity of other substrates remained similar (Fig. 1). The protonation of glutamate at the distal carboxylate forms a neutral amino acid and resembles more closely the structure of glutamine. The effective concentration of the protonated form of 1 mM glutamate at pH 6.0 is 30 μ M (based on the calculated pK_a of 4.57 for the distal acid group using ACD 6.0 software), implying that the protonated form of glutamate has a very high affinity for the

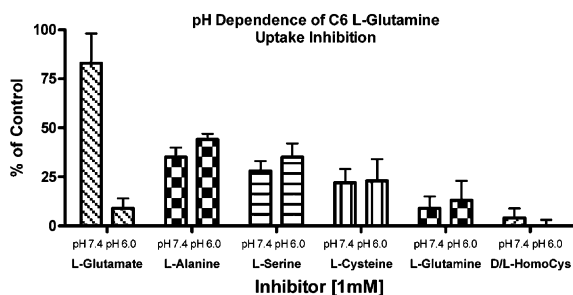


Figure 1. pH dependence of amino acid substrates on the ability to inhibit C6 glioma cell uptake of ³H-L-glutamine. While L-glutamate is somewhat inactive at pH 7.4, it becomes a potent inhibitor when the pH of the buffer is lowered to pH 6.0.

ASCT2 binding site. D/L-Homocysteine (–SH pK_a = 10.52) was found to be a more potent inhibitor of glutamine uptake, at pH 6.0 than L-glutamine (amide–NH pK_a = 16.52). These observations suggest that the distal group of the ligand may participate in a hydrogen bond donation that enhances the binding affinity of the ligand dramatically, and the more acidic the proton (without being fully ionized), the stronger the hydrogen bond. This hypothesized hydrogen bonding interaction may be a way to not only enhance the potency of the synthetic ligands, but to impart selectivity for the ASCT2 transporter over the other glutamine transporters.

Therefore, a key design feature of the synthetic analogues included a component to alter the pK_a of the glutamine amide NH to test the H-bonding hypothesis. It was anticipated, in support of this hypothesis, that lowering the pK_a of the amide NH would increase binding affinity to the ASCT2 transporter. In order to affect the acidity of the amide NH of L-glutamine, electron withdrawing and electron donating groups could be positioned such that the electronic effects could influence the stability of the resulting negative charge forming on the nitrogen. If substituents are placed directly on the nitrogen, effects other than electronic (i.e., steric, H-bonding, lipophilic, hydrophilic) may be the cause of activity changes. We decided to use the N-phenyl substitution as the template for altering the pK_a of the NH. By using this substitution, the conjugated ring allows more direct substituent effects on the nitrogen electronic density while not influencing the steric environment in the immediate NH vicinity.

Another important design feature of the synthetic analogues is the three-dimensional positioning of the functional groups. Since little is known about the 3-D requirements of binding to the ASCT2 transporter binding site, an acyclic template was decided upon. This would impart little conformational bias between the different N-phenyl substituted analogues and allow more direct analysis of the electronic effects of the substituents. Since glutamine has a slightly greater affinity for the ASCT2 transporter than asparagine,²⁰ the glutamine length template was used. Therefore, the synthetic analogue design to test the H-bond hypothesis was established as the substituted γ -N-phenyl L-glutamine derivative illustrated in Figure 2.

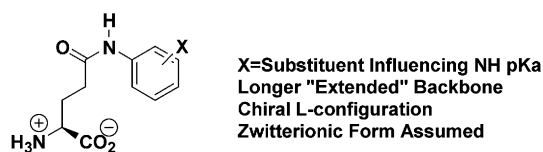


Figure 2. L-Glutamine analogue design. The substituents are electron donating and electron withdrawing which influence the acidity of the amide NH. This will test the proposed H-bond hypothesis at the ASCT2 transporter.

2. Results and discussion

The synthetic scheme to obtain the N-phenyl analogues used L-glutamic acid as the chiral starting material, following a reported sequence shown in Scheme 1.²⁶ Nitrogen protection of glutamic acid with benzyl chloroformate resulted in the diacid carbamate **1**. In order to differentiate the two carboxylic acid groups, the selective conversion to the azalactone **2** was performed in high yield. The resulting monoacid **2** was treated with thionyl chloride in refluxing methylene chloride to yield the acid chloride that was immediately treated with the desired aniline derivative in the presence of pyridine. This afforded the N-phenyl amide derivative **3**. Saponification of the lactone moiety was accomplished using lithium hydroxide, with subsequent deprotection of the carbamate using catalytic hydrogenation conditions, affording the desired γ -N-phenyl L-glutamine derivatives **4** in modest yield (combined deprotection yields: **5** 68%, **6** 65%, **7** 52%, **8** 63%, **9** 57%, **10** 45%, **11** 75%, **12** 71%, **13** 61%).

The N-aryl glutamine analogues shown in Figure 3 were tested for the ability to inhibit the uptake of tritiated glutamine in the C6 cell line at both pH 7.4 and 6.0 in the presence of the system L inhibitor BCH. The results shown in Table 1, noting the trend of increased ability to inhibit the uptake of tritiated glutamine with decreased pK_a (N–H) of the ligands **5–8**, support the H-bond hypothesis for the ASCT2 binding site; that the distal group of the ligand can participate in a hydrogen bond donation that will enhance the binding affinity of the ligand, and as the pK_a of the amide proton decreases, the hydrogen bond interaction increases.

To support the assumption that this effect in activity is due to an increased affinity for the transporter binding site, a kinetic analysis of the *p*-nitrophenyl anilide **8** was performed to determine the mechanism of inhibition. The concentration dependent inhibition curves were used to fit the classical Michaelis–Menten equation $v = V_{max}[S]/(K_{mapp} + [S])$ with $K_{mapp} = K_m (1 + [I]/K_i)$ by nonlinear regression (Fig. 4), where v is uptake velocity, $[S]$ is radiolabeled glutamine concentration, and $[I]$ is inhibitor concentration. On replotting the data to obtain a Lineweaver–Burk plot, the different lines intersect

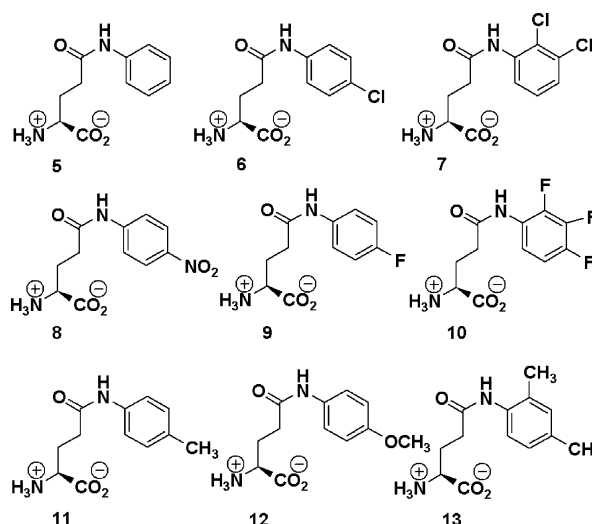
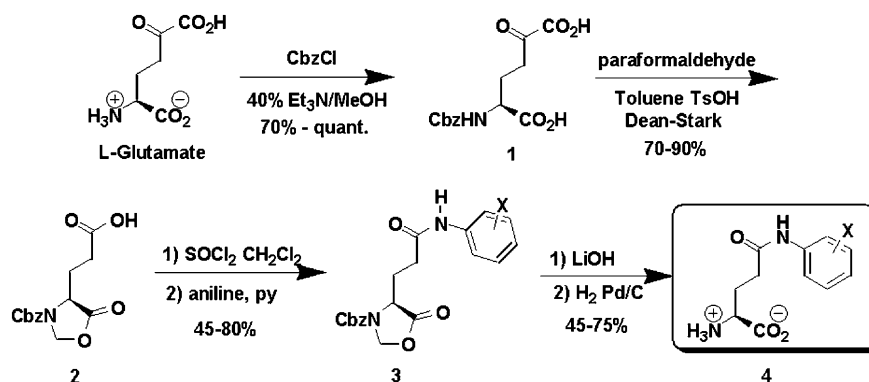


Figure 3. Synthetic glutamine analogues used to test the H-bond hypothesis of neutral amino acid transporter ASCT2.

on the y -axis, suggesting a competitive mechanism of inhibition and supporting the assumption that the effects of glutamine uptake inhibition result from ligand–protein bonding interactions in the transporter binding site. Presumably, the compounds act as reversible inhibitors of glutamine uptake by acting as alternative substrates. The actual transport of the analogues, however, has yet to be shown.

The glutamine uptake inhibition data in Table 1 shows a trend with respect to pK_a , but also show anomalous results. The analogues **11**, **12**, and **13** containing the electron donating groups on the phenyl ring were expected to show low glutamine uptake inhibition activity similar to that of the unsubstituted analogue **5**, based on similar pK_a (NH) values. On the contrary, these compounds were quite potent inhibitors of glutamine uptake at pH 6.0, suggesting lipophilic bonding interactions between ligand and protein occur within the binding site of the transporter. On the other side of electronic influence, the fluorophenyl analogues **9** and **10** were expected to show higher ability to inhibit the uptake of tritiated glutamine than the chlorophenyl analogues **6** and **7**, based on lower calculated pK_a (NH) values.



Scheme 1. Synthesis of L- γ -glutamyl anilide derivatives **4**.

Table 1. C6 L-glutamine uptake inhibition by synthetic analogues at pH 6.0 and 7.4

Synthetic analogues		Percent of control ^a ± SD		
Compound	p <i>K</i> _a (N–H) ^b	[Inhibitor] (mM)	pH = 7.4	pH = 6.0
5	15.00	1	61 ± 12	65 ± 13
		0.5	68 ± 1	76 ± 9
6	14.12	1	68 ± 15	1 ± 3
		0.5	62 ± 7	11 ± 2
7	13.40	1	53 ± 9	4 ± 8
		0.5	58 ± 3	4 ± 4
8	13.79	1	12 ± 13	0 ± 9
		0.5	13 ± 7	0 ± 15
		0.25	55 ± 14	15 ± 21
9	13.98	1	61 ± 8	61 ± 6
		0.5	77 ± 11	65 ± 12
10	12.11	1	59 ± 2	14 ± 3
		0.5	69 ± 2	42 ± 4
11	15.00	1	51 ± 5	0 ± 3
		0.5	74 ± 1	23 ± 7
12	15.01	1	55 ± 16	0 ± 6
		0.5	78 ± 6	40 ± 4
13	14.41	1	54 ± 3	0 ± 5
		0.5	69 ± 8	21 ± 4

^a 100% of control = 0.5–1.8 nmol/mg/min, incubation time = 5 min, $n \geq 3$ for all values, [³H-L-glutamine] = 100 μM.

^b p*K*_a calculations performed using ACD 6.0 software.

Kinetic Analysis of Glutamine Uptake Inhibition for Analogue 8 at pH 6.0 in C6 Cells

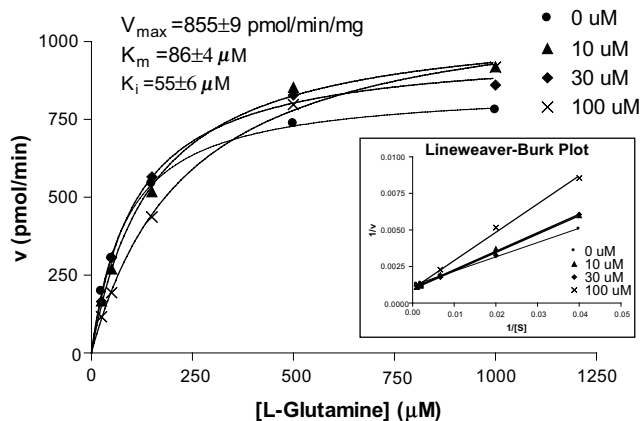


Figure 4. Inhibition curves for *p*-nitrophenyl glutamyl anilide **8** fit to Michaelis–Menten kinetics. Inset shows Lineweaver–Burk plot of same data to better illustrate competitive inhibition as lines converge at $1/[S] = 0$.

Surprisingly, these compounds were somewhat inactive at pH 6.0.

To help visualize these substituent effects, a Comparative Molecular Field Analysis (CoMFA) was performed. Using the Cheng–Prusoff relation, %inhib. = $[I]/([I] + K_i(1 + [S]/K_m))$, the K_i was estimated and used as the dependent variable. Since the only difference between

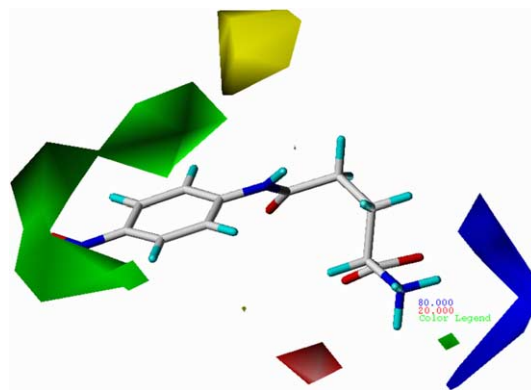
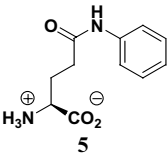
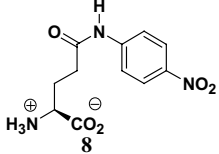
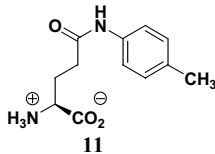
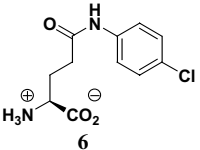
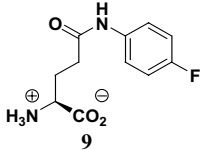
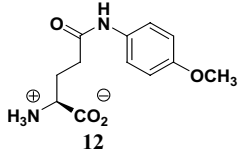
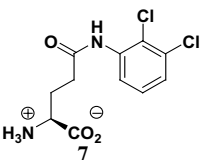
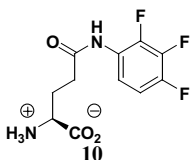
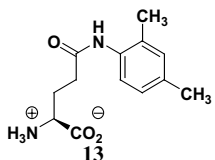


Figure 5. CoMFA with PLS STD*DEV COEFF shown. Steric addition in the green area should increase activity supporting a lipophilic pocket hypothesis, while steric addition in the yellow area should decrease activity, supporting a benefit in NH accessibility. The blue and red areas should enhance activity on increasing positive and negative charges, respectively.

analogues is the substitution at the amide nitrogen, the acyclic glutamine backbone was minimized and used as the template for each analogue and re-minimized, resulting in the same basic conformation for each analogue. This helps to focus the analysis on the substituent effects. Using the default parameters in the SYBYL 6.91 advanced computation module, the calculated steric, electronic, and CoMFA properties along with the calculated p*K*_a were compared to the estimated p*K*_i values. The resulting CoMFA model is shown in Figure 5. The volumes of space surrounding the molecule (the *p*-nitrophenyl derivative **8** shown) depict areas where molecular properties are predicted to increase affinity or decrease affinity for the protein. The green area around the aromatic ring is where adding steric bulk should increase ligand affinity (identifying a potential lipophilic pocket). The yellow area above the amide N–H is where adding steric bulk should decrease affinity, supporting the hypothesis that the protein may occupy this region and act as the hydrogen bond acceptor. The red region and the blue region support ionic interactions from the zwitterionic form of the analogues (which were initially used for the calculations).

Although the CoMFA model supports the H-bond hypothesis and identifies a possible lipophilic pocket, the model does not explain the low glutamine uptake inhibition activity of the fluorophenyl analogues **9** and **10** at pH 6.0. We believe that the increased anionic character of the fluorine atoms may have a destabilizing effect on bonding when positioned in this potential lipophilic pocket. To support this, log *D* (pH 6.0) values (partition coefficients between octanol and water of the ionic form at the corresponding pH) were calculated (using ACD 6.0 software) and compared (Table 2). The comparison does suggest a better solvation in water (a more negative value) of the fluoro analogues than the chloro analogues. A component making up the log *D* property, the H-bond acceptor ability, was also compared. Using the MOLCAD module of SYBYL 6.91, the H-bond acceptor surface was calculated and the surface

Table 2. Log *D* values calculated for the synthetic analogues at pH 6.0

Analogue	Log <i>D</i> ^a (pH 6.0)	Analogue	Log <i>D</i> (pH 6.0)	Analogue	Log <i>D</i> (pH 6.0)
	-1.79		-1.22		-1.33
	-0.82		-1.40		-1.78
	-1.00		-1.20		-0.87

On comparing the fluoro analogues **9** and **10** with the chloro analogues **6** and **7**, the fluoro analogues would appear to have a better solvation in water by the more negative value. On comparing the fluoro analogues **9** and **10** with the alkyl/alkoxy analogues **11**, **12**, and **13**, however, the fluoro analogues would appear to not be as well solvated in water.

^a Log *D* values calculated using ADC 6.0 software.

area of the molecule having H-bond acceptor property density of 0.02 or higher displayed (Fig. 6). The resulting H-bond acceptor surface area is significantly larger for the trifluorophenyl analogue **10**, than the other analogues analyzed. The *p*-fluorophenyl derivative **9** shows only a slight increase in H-bond acceptor surface area over the *p*-chlorophenyl compound **6**. Although the difference in H-bond acceptor surface area does not fully account for the dramatic decrease in glutamine uptake inhibition activity of compound **9**, these combined re-

sults suggest a stronger solvation of the fluorophenyl compounds in water. The lowered glutamine uptake inhibition activity seen by the fluoro compounds could be the result of the desolvation energy required to strip the waters off, while in binding to the protein there is no complimentary interaction to regain that solvation energy. This implies that within this region of space in the binding site, there are no hydrogen bond donors, supporting a lipophilic pocket.

3. Conclusion

Based on initial characterization, the ASCT2 H-bond hypothesis was proposed. Through the use of glutamine analogue probes, this hypothesis was supported and an additional bonding hypothesis was generated: a lipophilic pocket is in the binding site. These hypotheses are summarized in the graphic in Figure 7, illustrating

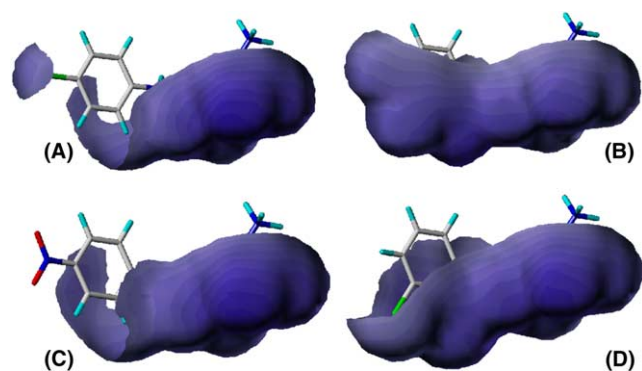


Figure 6. H-Bond acceptor surfaces for fluoro analogues **9** and **10** (A and B, respectively) and the potent inhibitors *p*-nitrophenyl glutamyl anilide **8** and 2,3-dichlorophenyl glutamyl anilide **7** (C and D, respectively). The surface is the H-bond acceptor density with a density value of 0.02 and greater for the property. The areas calculated (SYBYL 6.91 MOLCAD module) are: A Å² = 106.93, B Å² = 172.05, C Å² = 104.87, and D Å² = 155.19, suggesting the trifluoro analogue **10**, A has the most H-bond accepting surface of the four compounds, while the monofluoro compound **9**, B has less H-bond accepting surface than the dichloro analogue **7**, D and similar to **8**, C. The lack of activity can be explained by solvation effects for **10**, but not readily for **9** through this analysis.

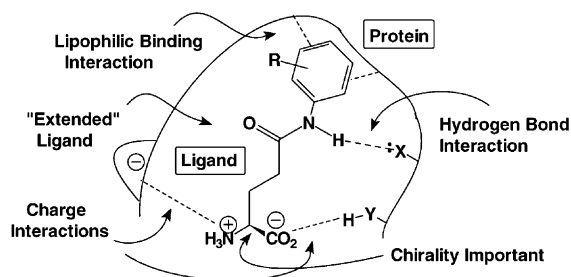


Figure 7. Preliminary neutral amino acid transporter ASCT2 binding site map based on the results of this study, illustrating the hydrogen-bond hypothesis and the lipophilic pocket hypothesis. Other features are also incorporated, such as an 'extended' conformation and the L-configuration.

a preliminary binding site map for the ASCT2 neutral amino acid transporter. Also through these experiments, a commercially available potent inhibitor of the ASCT2 transporter has been identified, the *p*-nitrophenyl analogue **8**. Although the fluorophenyl derivatives **9** and **10** fit within the parameters to suggest high potency glutamine uptake inhibition, these compounds are relatively inactive. This inactivity is explained by increased polarity of ring substituents resulting in a greater difference in solvation energy between bound and unbound states, supporting a lipophilic pocket in the binding site.

A recent set of experiments suggest that within the brain the S_N1 transporter (the system N isoform prominent in neuroglia) is the sole route for glial glutamine efflux involved in the recycling of glutamate neurotransmitter through the glutamine/glutamate cycle in the CNS.²⁴ This leaves the ASCT2 transporter function to be determined. One hypothesis is that the ASCT2 transporter functions as a facilitator of cellular needs, exchanging the abundant glutamine for deficient amino acids. The broad substrate profile supports this idea, and the up regulation in cancerous cells requiring an abundant variety of amino acids for the uncontrolled growth also lend to this hypothesis. Mentioned in a previous report,⁷ the pH dependent transport of glutamate by the ASC transport system offers an interesting possibility of aiding the clearance of synaptic glutamate. Provided the transporter is in the near vicinity of the vesicular glutamate release (accompanied by an acidic environment) a relevant contribution of glutamate uptake may be possible. As this project advances, new compounds may aid in identifying physiological roles of these transporters. We are currently looking at the 3-D preference of the functional groups, exploring the lipophilic pocket hypothesis, and investigating in more detail the hydrogen bonding hypothesis further in order to develop more potent and selective compounds to meet this end.

4. Experimental

4.1. General

L-[3,4³H(N)]-Glutamine was purchased from Perkin–Elmer and L- γ -nitrophenyl glutamyl anilide was purchased from ICN. D/L-Homocysteine, L-glutamate, anilines, and Cbz-chloride were purchased from ACROS Chemicals. NMR spectra were obtained on a Varian 400 MHz instrument using D₂O with acetonitrile in D₂O (δ 1.93 for proton, δ 1.3 for carbon) as the external standard, or DMSO with acetonitrile in DMSO as the external standard. Optical rotations were taken on a Perkin–Elmer polarimeter. HRMS were obtained through the Mass Spectrometry and Proteomics Core Facility, The University of Montana.

4.2. L-³H-glutamine analysis

The radiolabeled glutamine was analyzed for contamination by glutamate/pyroglutamate using paper chromatography by the method of Levintow and Meister³⁰ incorporating modifications by Khadem et al.³¹ The

L-³H-glutamine solution purchased from Perkin–Elmer was spotted lightly on Whatman No 4 filter paper cut into a strip 1 in. wide. A freshly prepared 1 mM glutamine solution in water was spotted adjacent to the label as a standard. The paper bottom is immersed in the mobile phase containing 70% *t*-butanol, 15% formic acid, 15% water, and 5 mg/mL ninhydrin (*R_f* values for L-glutamine, L-glutamate, and L-pyroglutamate in this solvent system are 0.22, 0.31, and 0.32, respectively). The addition of ninhydrin allows visualization of the glutamine standard on drying the chromatogram in air. After development, the chromatogram is dried in air and cut into ten or more numbered horizontal sections while noting where glutamine falls (identified by the standard). The individual sections are put into vials containing 1 mL water and allowed to soak for 30 min. The components are then quantified by the addition of 5 mL scintillation fluid and the radiation counted by scintillation counter. In most cases the radiolabel contained 10–15% contaminant, which was used without purification. Purification was performed by using tandem anion exchange/cation exchange cartridges (Whatman) and passing the volume of radiolabeled solution through using a syringe. After washing the resin with two volumes of deionized water, two volumes of 2 N ammonium hydroxide solution was passed only through the cation exchange cartridge. This effluent was lyophilized and taken up in one volume of deionized water.

4.3. Cell culture

C6 rat glioma cells were grown in Dulbecco's Modified Eagle Medium (Mediatech) (pH 7.4). The culture media was supplemented with 10% fetal calf serum and a mixture of penicillin (100 U/mL), streptomycin (100 mg/mL) and fungizone (0.1 mg/mL). All cell lines were cultured in 150 cm² flasks (Corning) and maintained at 37 °C in a humidified atmosphere of 5% CO₂. Cells were lifted from the flasks by the addition of trypsin (0.25% final concentration) for 3–5 min at 37 °C for passage every 7 days. At this time cell culture stocks for cryopreservation were prepared by maintaining 1 × 10⁶–2 × 10⁶ cells in the appropriate culture media supplemented with 20% FCS, 10% DMSO and storing at –196 °C under liquid N₂. Cells formed a confluent monolayer with an estimated density of 2.5 × 10⁶ cells and a protein concentration of 100–350 mg/well. Cells were given the appropriate fresh medium 2 h prior to an assay.

4.4. Cell culture glutamine transport assay

The C6 cell culture assays are carried out in 12-well plates.²⁷ Growth media is changed two hours prior to carrying out the uptake assay. Cellular assays are more consistent if the passage number does not exceed 60. Each set of conditions is carried out in triplicate, allowing for control uptake, two inhibitor experiments, and three samples for protein assay per plate. The wells at 31 °C are washed three times with 1 mL assay buffer at pH 6.0 or 7.4 (containing: 137 mM NaCl, 5.1 mM KCl, 0.77 mM KH₂PO₄, 0.71 mM MgSO₄·7H₂O, 1.1 mM CaCl₂, 10 mM D-glucose, 10 mM HEPES,)

and allowed to preincubate for 5 min in 1 mL buffer. The preincubation buffer is removed and ^3H -glutamine (100 μM , 500 λ) is added in same buffer (50 μL ^3H -Gln in 20 mL buffer) with 5 mM BCH and with or without inhibitor and allowed to incubate for 5 min. The radio-label is removed after 5 min, washed with 1 mL ice cold buffer three times, and lysed with 1 mL 0.4 N NaOH. After 24 h, 0.4 mL of the NaOH sample is put in a scintillation vial, 4 mL scintillation fluid is added, the sample is mixed and counted in a scintillation counter. All values are corrected for background by subtracting radioactivity accumulated in the presence of 10 mM glutamine for pharmacology experiments or at 0 °C using identical conditions for kinetic experiments, and reported as means \pm standard deviation of n assays. Protein concentrations for plates were sampled from three wells using the Pierce BCA (bicinchoninic acid) protein assay (Pierce, Rockford, IL).

4.5. Calculations

Physical properties ($\text{p}K_{\text{a}}$ and $\log D$ values) were calculated using ACD 6.0 software (Advanced Chemistry Development Inc., Toronto, Ontario, Canada M5H 3V9, <http://www.acdlabs.com>). Nonlinear regression was performed using GRAPHPAD PRISM version 4.00 for Windows (GRAPHPAD Software, San Diego California USA, <http://www.graphpad.com>). Kinetic data was fitted to Michaelis–Menten kinetics with data points equal to means \pm SD or SEM of n experiments having nonspecific binding subtracted, $n \geq 3$. Nonspecific binding measured as radiolabel retained in the presence of 10 mM unlabeled glutamine for pharmacology or at 0 °C for kinetics. All data were tested for significance using Student's t -test, and only results with $P < 0.05$ were considered to be statistically significant.

4.6. Molecular modeling

SYBYL 6.91 was used for molecular modeling calculations (Tripos Inc., <http://www.tripos.com>) on a Silicon Graphics O2 machine. Minimizations of the zwitterionic forms of the amino acid analogues used the following parameters: Tripos force field, Pullman charge calculation, dielectric constant = 80, minimization convergence criteria of 0.001 kcal/mol, Powell minimization method. CoMFA surfaces were calculated using SYBYL default parameters with $\text{p}K_{\text{i}}$ (K_{i} estimated from the relation $\% \text{inhib.} = [I]/([I] + K_{\text{i}}(1 + [S]/K_{\text{m}}))$ where $[I]$ is the inhibitor concentration, $[S]$ is the glutamine concentration, and $\% \text{inhib.} = 100 - \% \text{ of control}$ obtained in Table 1) as the dependent variable and $\text{p}K_{\text{a}}$, electronic, steric, and the SYBYL comfa measurement as the independent variables.

4.7. Chemistry

4.7.1. General procedure. 2-Benzyloxycarbonylamino-5-oxo-hexanedioic acid **1**: To 1 equiv L-glutamate in 40% triethylamine in methanol making a 1 M solution was added benzyl chloroformate neat and stirred for 3 h. The mixture was concentrated, diluted with water, and washed with diethyl ether. The aqueous layer was then

acidified to pH 2 with 6 N HCl, saturated with sodium chloride, and extracted with ethyl acetate three times. The combined ethyl acetate extracts were dried (MgSO_4), filtered, and concentrated to yield 70–98% pure L-Z-glutamate.

4-(2-Carboxy-ethyl)-5-oxo-oxazolidine-3-carboxylic acid benzyl ester **2**: To the **1** in toluene was added 1.5 equiv paraformaldehyde and 1% toluenesulfonic acid (wt/wt). The mixture was then refluxed under Dean–Stark conditions for approximately 3 h. The mixture was diluted with ethyl acetate and washed with brine, dried (MgSO_4), filtered, and concentrated to yield the Z-azalactone, which was used without further purification.

5-Oxo-4-(2-phenylcarbamoyl-ethyl)-oxazolidine-3-carboxylic acid benzyl ester **3**: To the anhydrous Z-azalactone **2** in methylene chloride (1 M solution) was added thionyl chloride and refluxed for 30 min at which time the reaction mixture was cooled to room temperature followed by the drop wise addition of 1 equiv aniline derivative and 1 equiv pyridine in methylene chloride. The mixture was stirred for an additional 15 min at room temperature, diluted with methylene chloride, and washed consecutively with 20% sodium phosphate pH 3.0 and saturated sodium bicarbonate solution. The organic solution was then dried with magnesium sulfate, filtered, and concentrated to yield the Z-azalactone amide **3**, which was used in the next step without further purification. The amide **3** was dissolved in a minimum of THF, chilled to 5 °C, and 1 equiv of a 1 M solution of LiOH added. The mixture was stirred for 30 min at which time the THF was removed by rotary evaporation. The remaining aqueous mixture was diluted with water, washed twice with ethyl acetate, then acidified to pH 2 with 6 N HCl, saturated with $\text{NaCl}_{(\text{s})}$, and extracted with ethyl acetate three times. The combined organic extracts were dried (MgSO_4), filtered, and concentrated to yield the pure N-Cbz carboxylic acid which was carried on to the next step without further purification.

N $_{\gamma}$ -Phenyl-glutamyl anilides **4**: The N-Cbz carboxylic acid was dissolved in methanol and the solution degassed by evacuation and flushing with argon. Palladium on carbon (10% Pd) was added to the methanolic solution (10% wt/wt), the mixture purged with hydrogen several times, and stirred under an atmosphere of hydrogen until no starting material remained by TLC. The reaction was filtered and the catalyst washed with water and additional methanol. The methanol was removed in vacuo and the water removed by rotary evaporation without heating or by lyophilization to yield pure glutamine derivative **4**.

The phenyl analogue and all mono-substituted derivatives (**5**, **6**, **8**, **9**, **11**, and **12**)^{25,28,29} match reported spectra.

L- γ -N-2,3-Dichlorophenyl glutamyl anilide **7**: ^1H NMR (DMSO): δ 7.28–7.36 (m, 3H), 4.01 (ddd, $J = 4.4, 4.5, 8.6$ Hz, 1H), 2.48 (m, 2H), 2.07 (m, 1H), 1.83 (m, 1H). ^{13}C NMR (DMSO): δ 173.8, 170.9, 137.1, 128.5,

128.0, 127.9, 126.7, 125.1, 53.4, 32.3 26.5. $[\alpha]_{\text{D}} +25.0$ (*c* 1.03); HRMS Calcd for $\text{C}_{11}\text{H}_{13}\text{N}_2\text{O}_3\text{Cl}_2 = 291.0303$. Found 291.0308.

L- γ -N-2,3,4-Trifluorophenyl glutamyl anilide **10**: ^1H NMR (DMSO): δ 8.56 (br d, 2H), 7.55 (ddd, $J = 61.5$, 9.1, 5.2 Hz, 1H), 7.19 (ddd, $J = 86$, 8.74, 4.85 Hz, 1H), 3.89 (br, 1H), 2.60–2.35 (2dd, $J = 8.4$, 9.0 Hz, 2H), 2.11 (dd, $J = 5.8$, 5.8 Hz, 1H), 2.01 (dd, $J = 5.8$, 5.8 Hz, 1H). ^{13}C NMR (DMSO): δ 173.7, 170.9, 152.1 ($J = 260$ Hz), 141.3 ($J = 260$ Hz), 138.14 ($J = 260$ Hz), 123.0, 119.0, 111.7, 53.3, 32.1, 26.4. $[\alpha]_{\text{D}} +25.4$ (*c* 1.32); HRMS Calcd for $\text{C}_{11}\text{H}_{12}\text{N}_2\text{O}_3\text{F}_3 = 277.0800$. Found 277.0821.

L- γ -N-2,4-Dimethylphenyl glutamyl anilide **13**: ^1H NMR (D_2O): δ 6.96 (br s, 1H), 6.89 (s, 2H), 3.91 (t_{app} , $J = 6.7$ Hz, 1H), 2.50 (m, 2H), 2.11 (m, 5H), 1.95 (s, 3H). ^{13}C NMR (D_2O): δ 173.9, 172.0, 138.1, 131.4, 127.3, 126.8, 52.6, 31.3, 25.9, 20.2, 16.9. $[\alpha]_{\text{D}} +24.1$ (*c* 0.80); HRMS Calcd for $\text{C}_{13}\text{H}_{19}\text{N}_2\text{O}_3 = 251.1409$. Found 251.1396.

Acknowledgements

We would like to give a special thanks to Whitney Widhalm for all her efforts in helping the project along, Erin M. O'Brien for her help with cell culture, Professor Richard Bridges, Director of the Center for Structural and Functional Neuroscience, for his input and suggestions, Professor John Gerdes, Director of the Molecular Computational Core Facility, and the Department of Chemistry, The University of Montana and NSF for the use of the NMR instrument. This research was made possible by NIH Grant number P20 RR15583 from the COBRE Program of the National Center for Research Resources.

References and notes

- Johansen, L.; Roberg, B.; Kvamme, E. *Neurochem. Res.* **1987**, *12*, 135–140.
- J. Nutr.* **2001**, *131*, Suppl. 9, 2447S–2590S.
- Rennie, M. J.; Hundal, H. S.; Babij, P.; MacLennan, P.; Taylor, P. M.; Watt, P. W.; Jepson, M. M.; Millward, D. *J. Lancet* **1986**, *2*, 1008–1012.
- Boelens, P. G.; Nijvelde, R. J.; Houdijk, A. P. J.; Meijer, S.; Van Leeuwen, P. A. M. *J. Nutr.* **2001**, *131*, 2569S–2577S.
- Labow, B. I.; Souba, W. W. *World J. Surg.* **2001**, *24*, 1503–1513.
- Chaudhry, F. A.; Reimer, R. J.; Krizaj, D.; Barber, D.; Storm-Mathisen, J.; Copenhagen, D. R.; Edwards, R. H. *Cell* **1999**, *99*, 769–780.
- Varoqui, H.; Zhu, H.; Yao, D.; Ming, H.; Erickson, J. D. *J. Biol. Chem.* **2000**, *275*, 4049–4054.
- Bode, B. P.; Souba, W. W. *J. Parenter. Enteral Nutr.* **1999**, *23*, S33.
- Haussinger, D. *Metabolism* **1989**, *38*, 14–17.
- Bourke, E.; Haussinger, D. *Contrib. Nephrol.* **1992**, *100*, 58–88.
- Deitmer, J. W.; Broer, A.; Broer, S. *J. Neurochem.* **2003**, *87*, 127–135.
- Rae, C.; Hare, N.; Bubb, W. A.; McEwan, S. R.; Broer, A.; McQuillan, J. A.; Balcar, V. J.; Conigrave, A. D.; Broer, S. *J. Neurochem.* **2003**, *85*, 503–514.
- Broer, S.; Brookes, N. *J. Neurochem.* **2001**, *77*, 705–719.
- Chaudhry, F. A.; Schmitz, D.; Reimer, R. J.; Larsson, P.; Gray, A. T.; Nicoll, R.; Kavanaugh, M.; Edwards, R. H. *J. Neurosci.* **2002**, *22*, 62–72.
- Bode, B. P. *J. Nutr.* **2001**, *131*, 2475S–2485S.
- Zerangue, N.; Kavanaugh, M. P. *J. Biol. Chem.* **1996**, *271*, 27991–27994.
- Broer, A.; Brookes, N.; Ganapathy, V.; Dimmer, K. S.; Wagner, C. A.; Lang, F.; Broer, S. *J. Neurochem.* **1999**, *73*, 2184–2194.
- Utsunomiya-Tate, N.; Endou, H.; Kanai, Y. *J. Biol. Chem.* **1996**, *271*, 14883–14890.
- Dolinska, M. D. A.; Hilgier, W.; Zielinska, M.; Zablocka, B.; Buzanska, L.; Albrecht, J. *J. Neurosci. Res.* **2001**, *66*, 959–966.
- Wasa, M.; Wang, H. S.; Okada, A. *Am. J. Physiol. Cell. Physiol.* **2002**, *282*, C1246–C1253.
- Dolinska, M.; Dybel, A.; Albrecht, J. *Neurochem. Int.* **2000**, *37*, 139–146.
- Dolinska, M.; Dybel, A.; Zablocka, B.; Albrecht, J. *Neurochem. Int.* **2003**, *1353*.
- Li, R. Y. M.; Frolov, A.; Wheeler, T. M.; Scardino, P.; Otori, M.; Ayala, G. *Anticancer Res.* **2003**, *23*, 3413–3418.
- Boulland, J. L.; Osen, K. K.; Levy, L. M.; Danbolt, N. C.; Edwards, R. H.; Storm-Mathisen, J.; Chaudhry, F. A. *Eur. J. Neurosci.* **2002**, *15*, 1615–1631.
- Parker, C. M.-B. E.; Meehan, G.; Piva, T.; Rigano, D.; Favot, P.; West, M.; McCabe, M. G. P.; Miller, D. J. World Patent 9,003,399, 1990.
- Lee, B. H.; Miller, M. J. *Tetrahedron. Lett.* **1984**, *25*, 927–930.
- Bridges, R.; Stanley, M. S.; Anderson, M. W.; Cotman, C. W.; Chamberlin, A. R. *J. Med. Chem.* **1991**, *34*, 717–725.
- Menard, A. C. R.; Lherbet, C.; Rivard, C.; Roupioz, Y.; Keillor, J. W. *Biochemistry* **2001**, *42*, 12678–12685.
- Huang, X.; Luo, X.; Roupioz, Y.; Keillor, J. W. *J. Org. Chem.* **1997**, *62*, 8821.
- Levintow, L.; Meister, A. *J. Biol. Chem.* **1954**, *209*, 265.
- El Khadem, H. S.; El-Shafei, Z. M.; Abdel Rahman, M. M. A. *Anal. Chem.* **1963**, *35*, 1766.